

Supporting Information

Gas-template directed *in-situ* synthesis of highly nitrogen-doped carbon nanotubes with superior sulfur compatibility and enhanced functionalities

Xun Kan,^{†a} Jinxing Mi,^{†a} Yong Zheng,^{*a,b} Yihong Xiao,^{a,b} Fujian Liu^{*a,b} and Lilong Jiang^{a,b}

^a National Engineering Research Center of Chemical Fertilizer Catalyst (NERC-CFC), School of Chemical Engineering, Fuzhou University, Gongye Street 523#, Fuzhou, 350002, China.

E-mail: zhengyong@fzu.edu.cn, fjliu@fzu.edu.cn

^b State Key Laboratory of Catalysis, Dalian Institute of Chemical Physics, Chinese Academy of Sciences, Dalian 116023, China.

[†]These authors contribute equally to this work.

Experimental

Chemicals and reagents

All the chemicals were analytical grade and used directly without further purification. Glucose (99.0 wt.%) and urea (99.0 wt.%) were purchased from Sigma-Aldrich Co., Ltd. The gases used in this work, including H₂S (99.99 vol.%), mixed gases of H₂S and O₂ (composition: 5000 ppm H₂S, 2500 ppm O₂, balanced in N₂), and mixed gases of H₂S and N₂ (composition: 50 000 ppm H₂S, balanced in N₂) were supplied by Dalian Special Gas Company. For comparison, commercial nitrogen-doped carbon nanotubes (C-N-CNTs) and commercial carbon nanotubes (C-CNTs) were purchased from XFNANO Co., Ltd.

Preparation of samples

The N-MWCNTs materials were prepared from one-step controllable carbonization of solid raw materials of glucose and 12.0 g of urea. Typically, 2.0 g of glucose and 12.0 g of urea were homogeneously mixed via manual grinding for 5 min. Subsequently, the mixture was transferred into a quartz crucible (3×12 cm) which was placed in a tubular furnace, and subject to controllable carbonization in a flow of N₂. The thermal treatment was heating to 900 °C at a rate of 2.5 °C/min, and calcining at 900 °C for 1 h. After cooling to room temperature, the nitrogen-doped multi-walled carbon nanotubes (denoted herein as N-MWCNTs) distributed in flocculent appearance on the inside wall of the quartz crucible were harvested.

Characterizations

X-ray diffraction (XRD) measurements were performed on an X'Pert3 Powder diffractometer using Cu K α radiation (40 mA, 45 kV). Laser Raman spectra were recorded on a Renishaw InVia Reflex spectrometer at wavelength of 532 nm (100 mW). Specific BET surface areas and pore volumes were determined from N₂ adsorption-desorption isotherms at -196 °C using a Micromeritics ASAP 2020M system, the sample was degassed under vacuum (1×10^{-5} Pa) at 180 °C for 6 h prior to measurement. X-ray photoelectron spectroscopic (XPS) analysis was performed on a Thermo Fisher Scientific EscaLab 250Xi spectrometer. Scanning electron microscopic (SEM) analysis was performed on S-4800 Hitachi with an accelerating voltage of 5 kV. Transmission electron microscopy (TEM) images were collected on a Zeiss Libra200 TEM at an acceleration voltage of 200 kV.

Photoemission spectroscopy experiments and Near Edge X-ray Absorption Fine Structure (NEXAFS) were carried out at the Catalysis and Surface Science Endstation at the BL11U beamline in the National Synchrotron Radiation Laboratory (NSRL) in Hefei, China.

The beamline was connected to an undulator and equipped with two gratings that offer soft X-rays from 20 to 600 eV with a typical photon flux of 5×10^{10} photons/s and a resolution($E/\Delta E$) better than 105 at 29 eV. This system was comprised of four ultrahigh vacuum (UHV) chambers including analysis chamber, preparation chamber, molecular beam epitaxy (MBE) chamber, and a radial distribution chamber. The base pressures were 7×10^{-11} , 1×10^{-10} , 5×10^{-10} and 2×10^{-11} mbar, respectively. A sample load-lock system was connected to the sample transfer chamber. The analysis chamber

was equipped with a VG Scienta R4000 analyzer, a monochromatic Al Ka X-ray source, a UV light source, low energy electron diffraction (LEED), a flood electron gun, and a manipulator with high precision and five-degree-of-freedom. The preparation chamber was comprised of an ion gun, a quartz crystal microbalance (QCM), a residual gas analyzer, a manipulator with high precision and four-degree-of-freedom, and several evaporators. The MBE chamber housed a QCM, several evaporators and a manipulator with two-degree-of-freedom. With this radial distribution chamber, the time for each transfer process between two chambers was less than 1 min.

Selective catalytic oxidation of H₂S

Selective catalytic oxidation of H₂S over the N-MWCNTs and C-N-CNT samples was performed in a continuous flow fixed-bed reactor at atmospheric pressure. Typically, 0.1 g of catalyst (100–120 mesh) was placed in the central section of the reactor. A gas mixture containing 5000 ppm of H₂S, 2500 ppm of O₂, and balance gas (N₂) was introduced into the reactor at a total flow rate of 20 mL/min (WHSV=12 000 mL g⁻¹ h⁻¹), with reaction performed in the temperature range of 90–210 °C. After reaction, the effluent stream was analyzed by a gas chromatograph (GC9790II) equipped with a FPD and a TCD (thermal conductivity detector). A condenser was placed at the bottom of the reactor to trap sulfides in the effluent stream to avoid pollution. Instantaneous fractional conversion of H₂S, sulfur selectivity, and sulfur yield are defined as follows:

$$\text{H}_2\text{S conversion} = \frac{(\text{H}_2\text{S})_{\text{in}} - (\text{H}_2\text{S})_{\text{out}}}{(\text{H}_2\text{S})_{\text{in}}} \times 100\% \quad (1)$$

$$\text{Sulfur selectivity} = \frac{(\text{H}_2\text{S})_{\text{in}} - (\text{H}_2\text{S})_{\text{out}} - (\text{SO}_2)_{\text{out}}}{(\text{H}_2\text{S})_{\text{in}} - (\text{H}_2\text{S})_{\text{out}}} \times 100\% \quad (2)$$

Meanwhile, the used N-MWCNTs can be regenerated by treating with flowing nitrogen at 300 °C for 6 h for removal of the surface deposited sulfur product.

Gas adsorption and separation

Prior to measurements, the samples were degassed in vacuum at 150 °C for 12 h. The H₂S adsorption isotherms were collected on a self-made equipment, the accuracy of which was validated in our previous work.^{S1} The equipment was mainly composed of two stainless steel chambers connected to two pressure transducers respectively. The amounts of adsorbed H₂S could be calculated according to the changing of the pressure of the two chambers as the samples were fully exposed to H₂S.

The breakthrough test for H₂S/N₂ (5 vol.%/95 vol.%) gas mixture over different samples were performed on a Micromeritics AutoChem II 2920 analyzer connected to a Hiden HPR-20 R&D mass spectrometer. All the measurements were conducted using a U-type quartz tube (6 mm inner diameter × 190 mm length). As a typical run, 100 mg of the sample was filled into the quartz tube and purged with a helium (He) flow (10 mL/min) at 80 °C for 3 h to remove any volatile impurities before the measurement. After the sample was cooled to 25 °C, the He flow was switched to a H₂S/N₂ mixed gas flow (10 mL/min) for evaluating the competitive adsorption. The composition of inlet

gas was controlled by mass flowmeters. The composition of outlet gas was measured online by the mass spectrometer.

Li-S battery

The obtained N-MWCNTs was mixed with sulfur in a mass ratio of 3:1, then the mixture was encapsulated in a small hydrothermal axe under dry N₂ in a glove box and then transferred into a drying box at 155 °C for 12 h. The electrodes were prepared by first blending 80 wt.% as-prepared composite materials, 10 wt.% acetylene carbon black, and 10 wt.% poly(vinylidene fluoride) binder (PVDF, (CH₂CF₂)_n, Sigma-Aldrich) in N-methyl-2-pyrrolidone (NMP, C₅H₉NO, Sigma-Aldrich, 99.5%) to form a slurry. The slurry was then pasted onto a piece of aluminum foil and dried in a vacuum oven for 12 h at 55 °C, which was subjected to pressing at 200 kg/cm². The mass loading of each electrode was ≈1.1 mg cm⁻¹. Electrochemical measurements were carried out using CR2032 coin cells with lithium foil as reference and counter electrode, and a porous polypropylene (Celgard 2300) as separator. The CR2032 coin cells were assembled in an argon-filled glove box (UniLab, Mbraun, Germany) with low levels of H₂O and O₂ (H₂O < 0.01 ppm, O₂ < 0.01 ppm). The electrolyte solution was 1 M LiTFSI and 1 wt.% LiNO₃ in 1,3-dioxolane and 1,2-dimethoxyethane (volume ratio 1:1). The galvanostatic charge–discharge measurements were performed at room temperature at different current densities in the voltage range of 1.7 to 2.6 V. Capacity-voltage (CV) from 1.7 to 2.6 V was carried out on a CHI 660 C electrochemistry workstation with a scan rate of 0.1 mV s⁻¹.

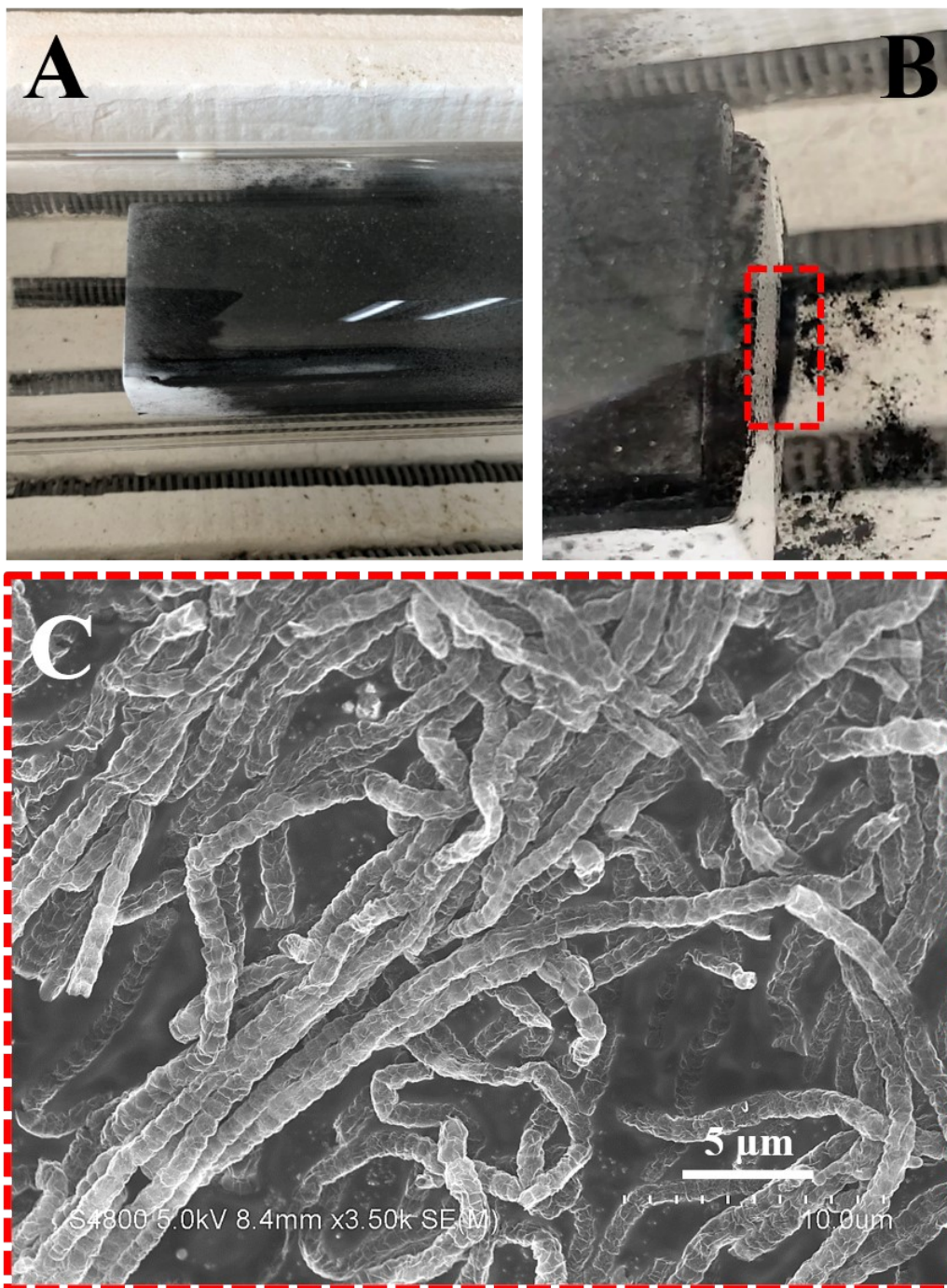


Figure S1. Photographs of N-MWCNTs (A and B); Corresponding SEM image of N-MWCNTs (C).

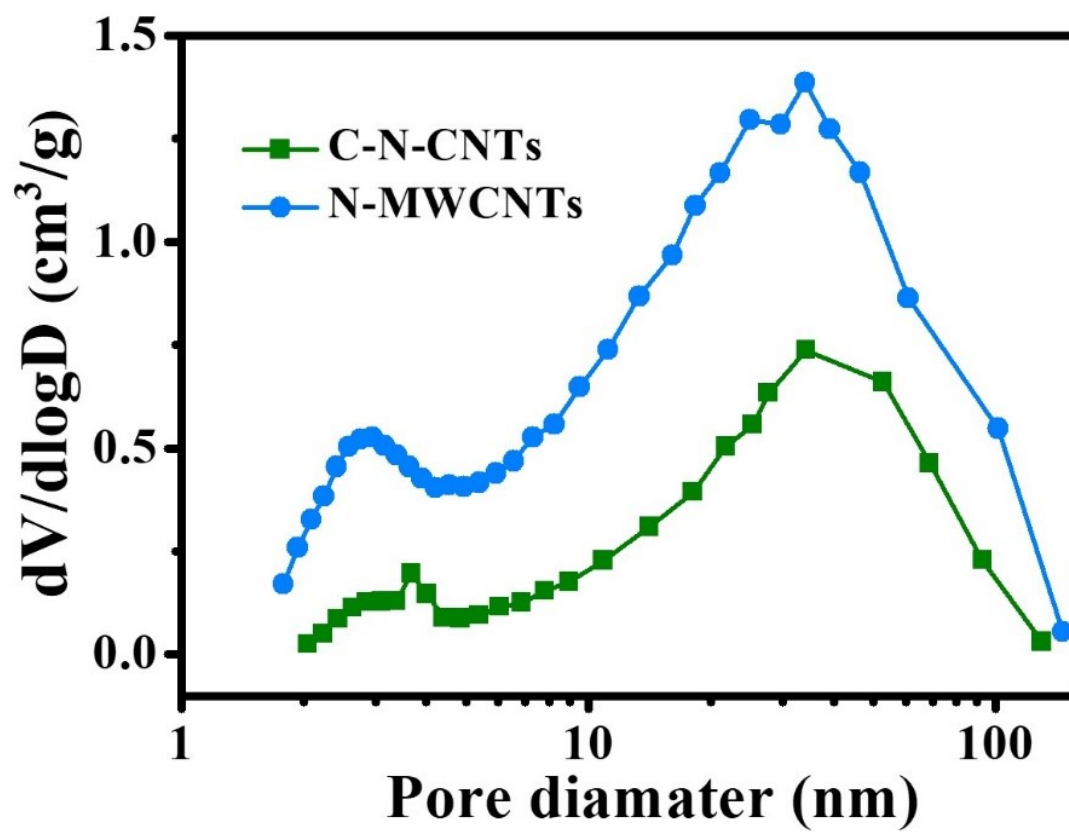


Figure S2. Pore size distribution curves of C-N-CNTs and N-MWCNTs.

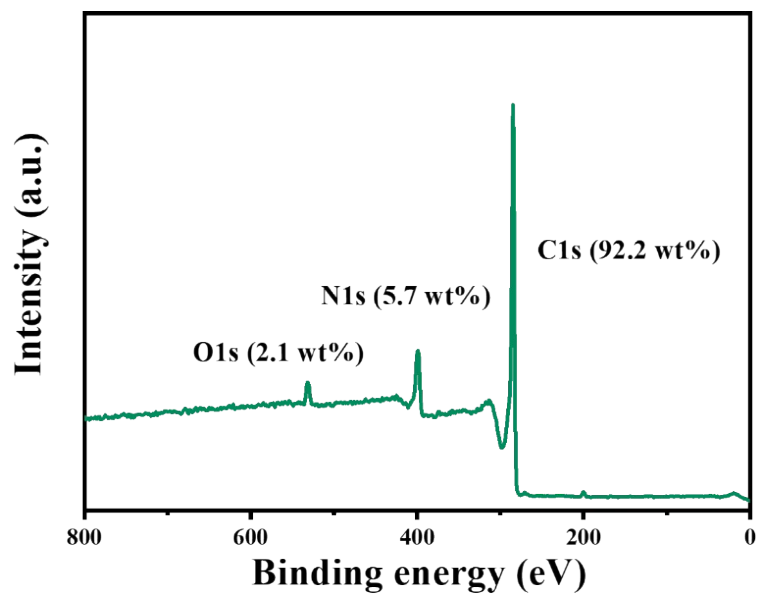


Figure S3. Survey XPS spectra of N-MWCNTs.

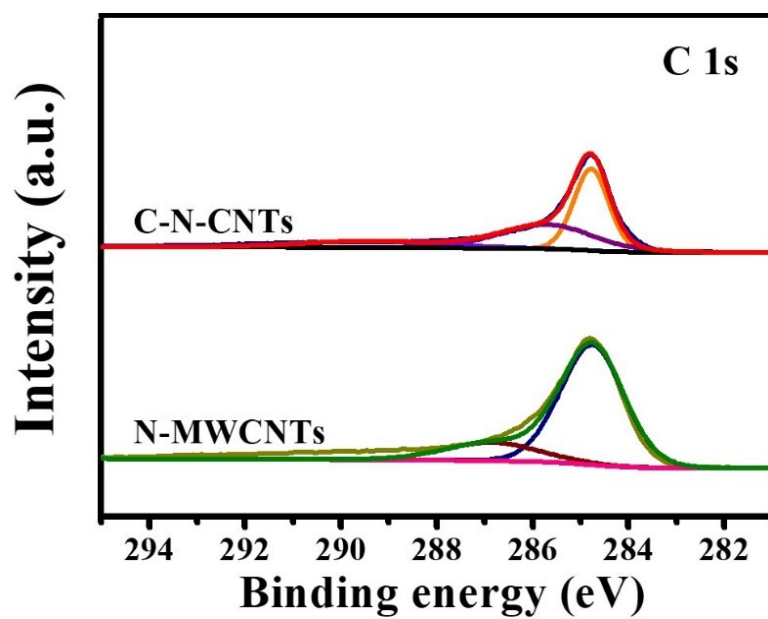


Figure S4. C1s XPS spectra of N-MWCNTs and C-N-CNT samples.

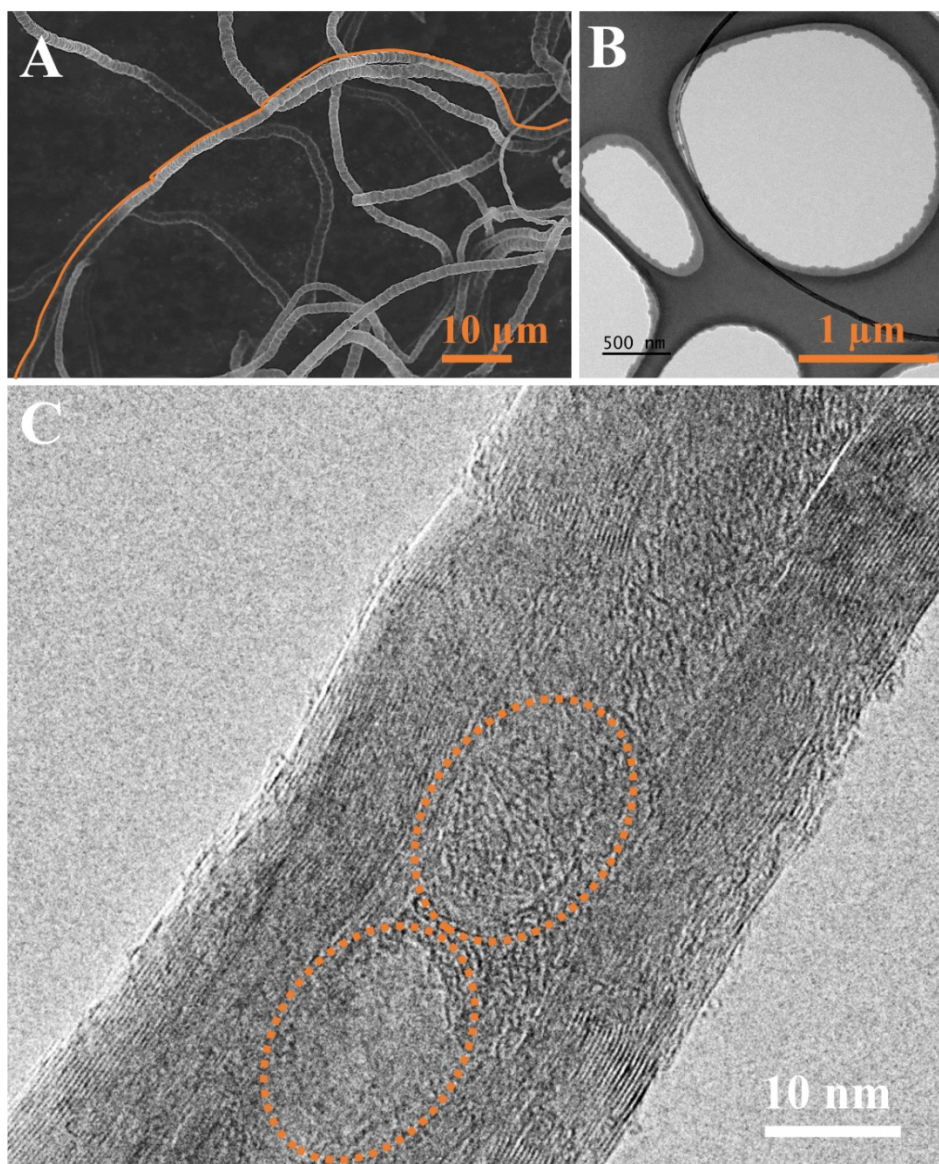


Figure S5. (A) SEM, and (B, C) TEM images of N-MWCNTs with bamboo-like structures.

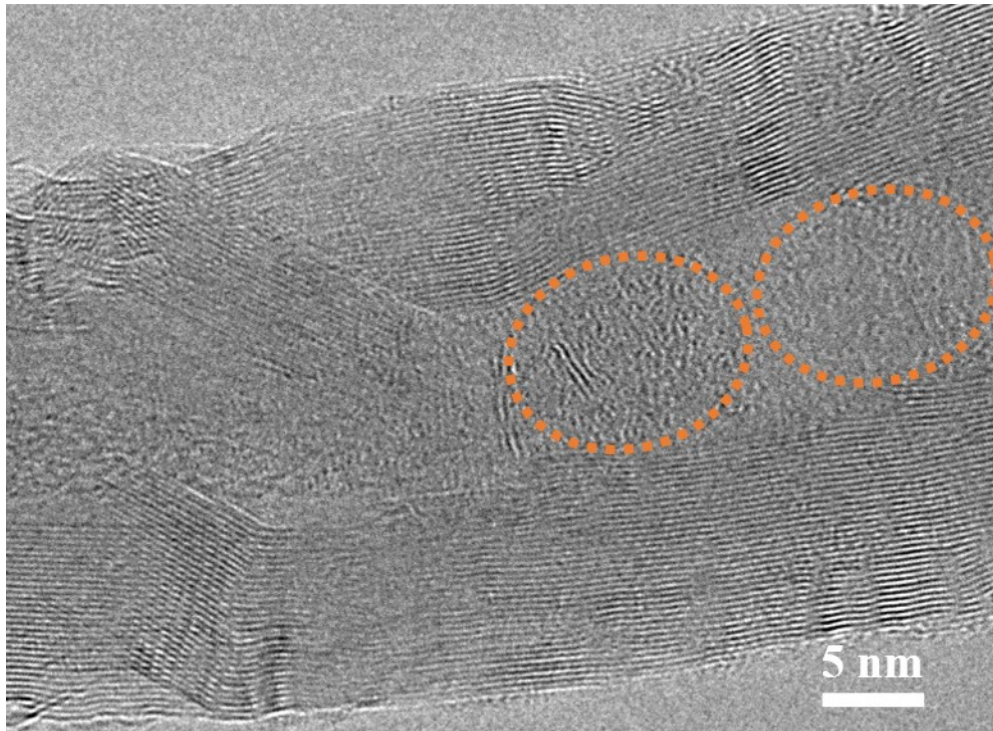


Figure S6. TEM images of N-MWCNTs with highly oriented features.

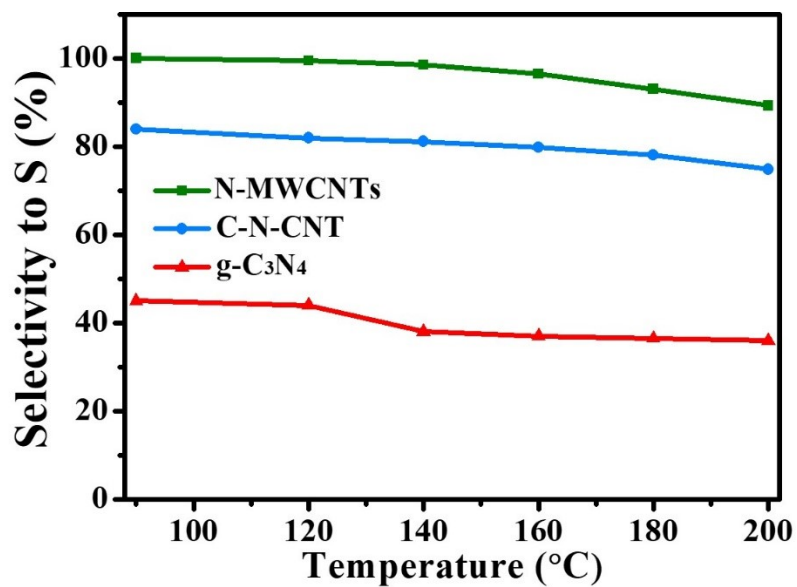


Figure S7. Sulfur selectivity over N-MWCNTs, C-N-CNTs, and g-C₃N₄ in H₂S selective oxidation versus temperature.

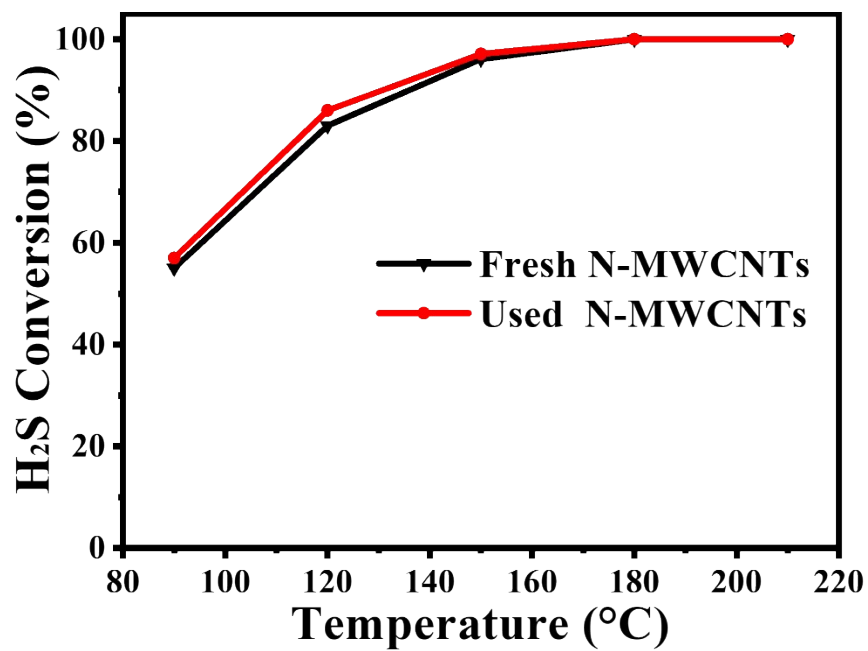


Figure S8. H₂S conversion curves on reaction temperature over various catalysts.

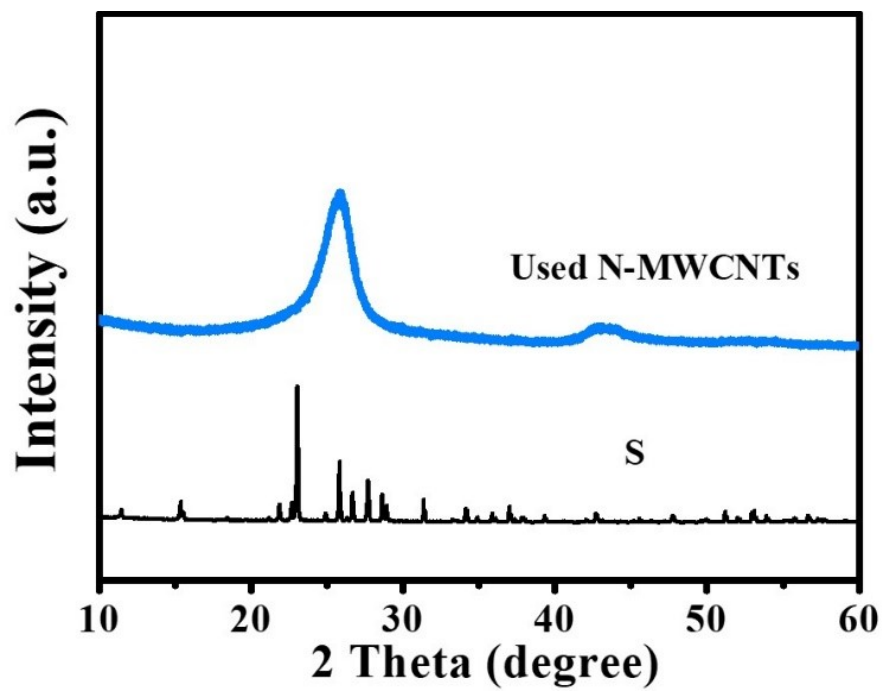


Figure S9. XRD pattern for the N-MWCNTs sample used in H₂S selective oxidation; also shown is the XRD pattern of elemental sulfur.

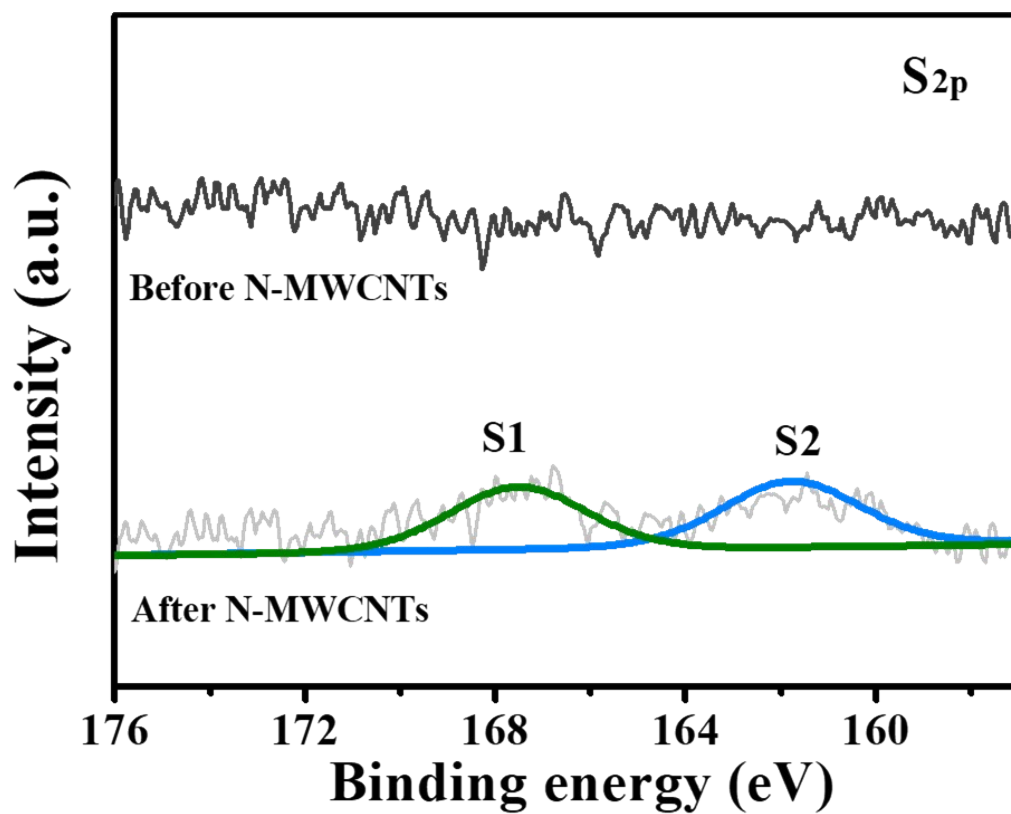


Figure S10. S_{2p} XPS spectra of N-MWCNTs sample before and after selective catalytic oxidation of H₂S.

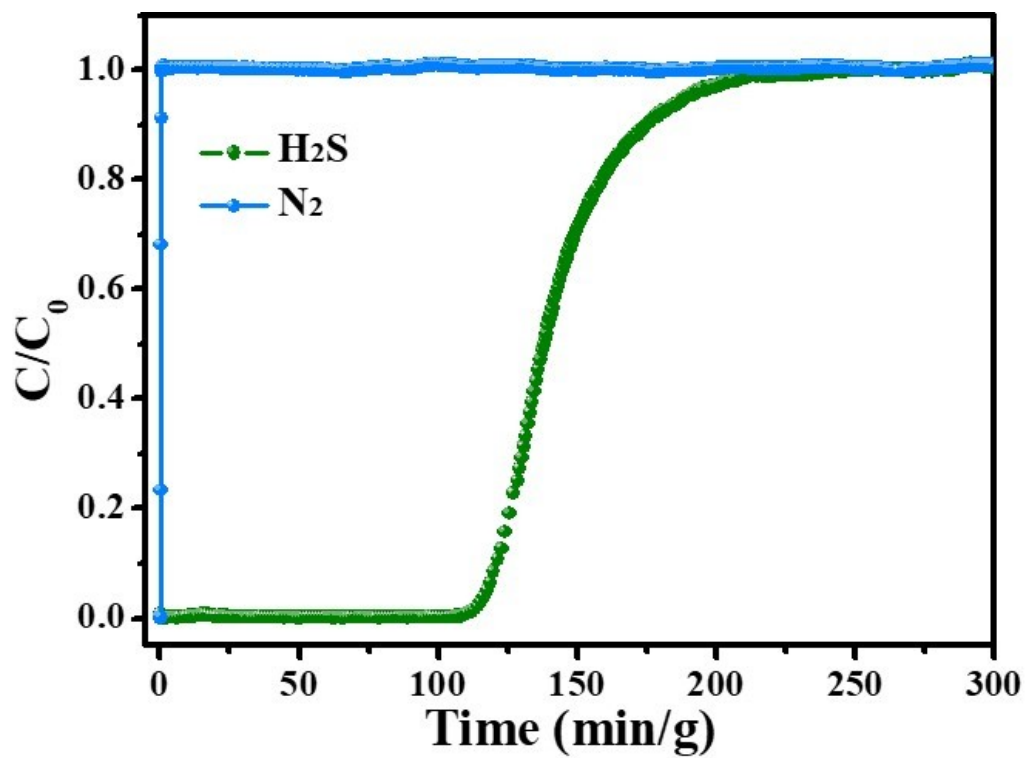


Figure S11. Breakthrough curves of N-MWCNTs for H_2S/N_2 gas mixture (10 mL/min) at 25 °C.

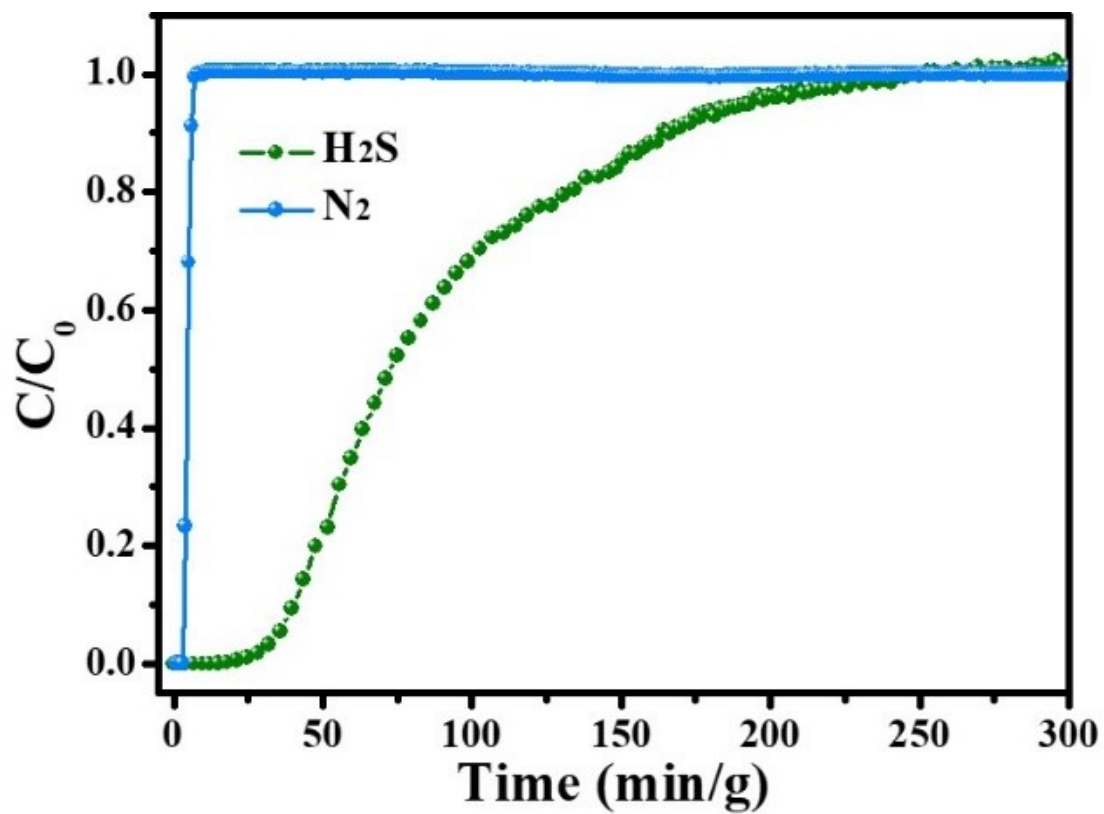


Figure S12. Breakthrough curves of C-N-CNT for H_2S/N_2 gas mixture (10 mL/min) at 25 °C.

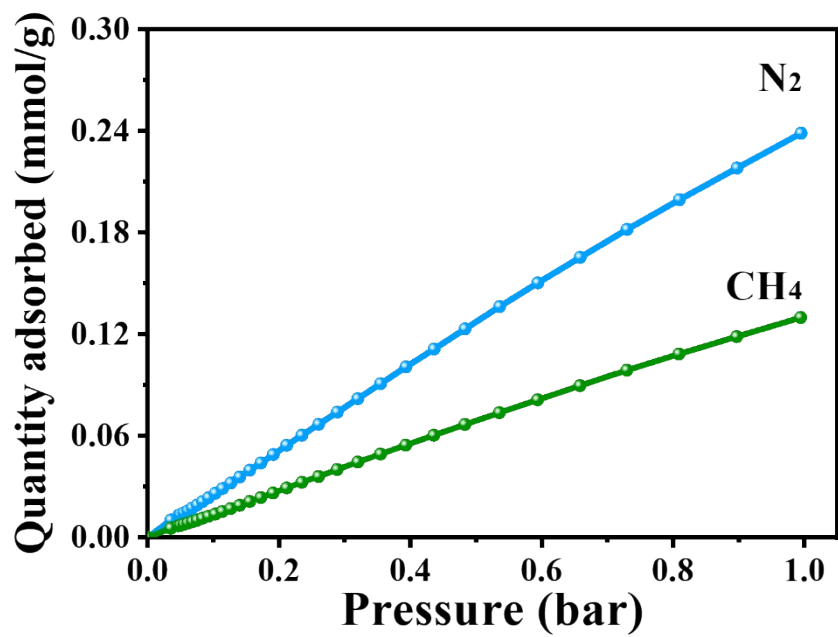


Figure S13. N₂ and CH₄ adsorption isotherms of N-MWCNTs at 25 °C and 1 bar.

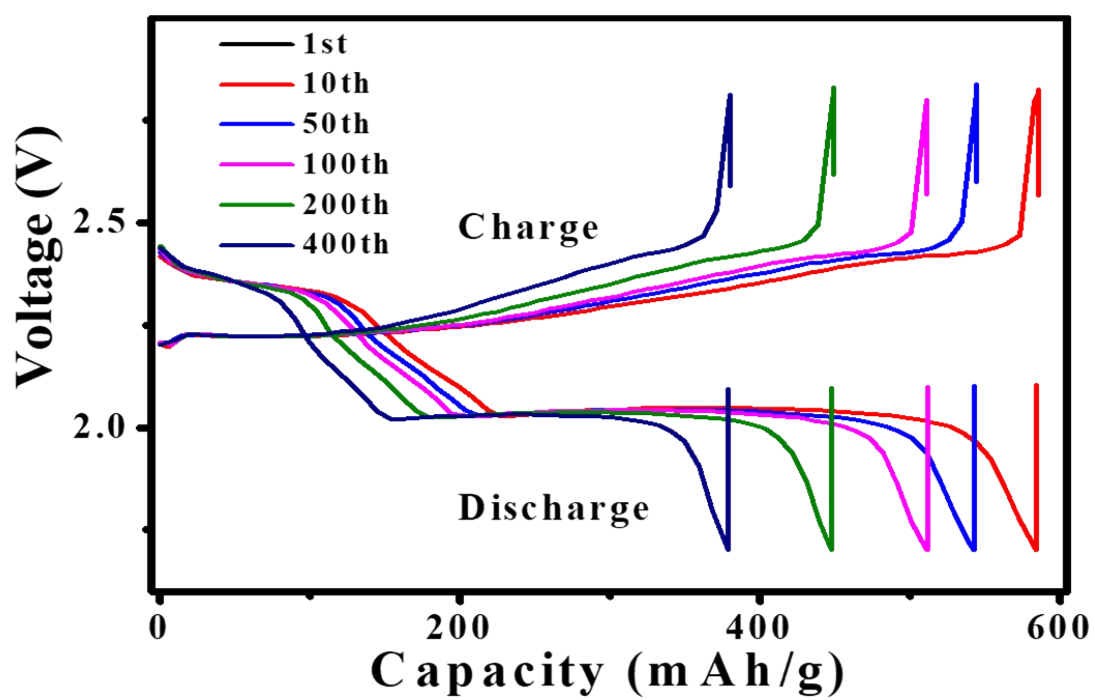


Figure S14. Galvanostatic charge and discharge (GCD) profiles of N-MWCNTs at 2.0

C.

Table S1 Structural characteristics of N-MWCNTs and C-N-CNT samples.

Catalyst	N (wt.%) ^[a]	S _{BET} (m ² /g) ^[b]	pore sizes (nm) ^[c]	V _m (cm ³ /g) ^[d]
N-MWCNTs	5.68	472	34.0	1.47
C-N-CNT	2.03	154	34.2	0.63

[a] Calculated from XPS results; [b] BET surface areas; [c] Estimated from BJH analysis; [d] V_m was obtained from the *t*-plot method

Table S2 H₂S adsorption capacities of N-MWCNTs and variously reported porous solid adsorbents.

Samples	Condition	H ₂ S capacities (mg/g)	Ref.
N-MWCNTs	50 000 ppm H ₂ S, N ₂ balance, 25 °C	106.8	This work
GO (5%)/HKUST	1000 ppm H ₂ S, air, 25 °C	3.9	S2
MIL-125-NH ₂ (Ti)	1% H ₂ S, N ₂ balance, 25 °C	7.9	S3
MIL-101 (Cr)-HNO ₃ -1	1% H ₂ S, He balance, 25 °C	10.1	S4
Cu/UiO-167	1000 ppm H ₂ S, air, 25 °C	11.5	S5
Zeolite 4A	1000 ppm H ₂ S, N ₂ balance, 50 °C	8.36	S6
0.15-CoX-600	1000 ppm H ₂ S, N ₂ balance, 25 °C	4.42	S7
13X Ex-Cu	1000 ppm H ₂ S, N ₂ balance, 120 °C	40.12	S8
20Zn-NaA	200 ppm H ₂ S, N ₂ balance, 28 °C	15.75	S9
Cu-ETS-2	10 ppm H ₂ S, He balance, 25 °C	29.7	S10
5-TiO ₂ /zeolite	35% N ₂ , 65% CH ₄ , dry, 0.1% H ₂ S, 25 °C	4.43	S11
Fe-NaA	1% H ₂ S, N ₂ balance, 30 °C	15	S12

References

- (S1) X. Kan, G. Zhang, Y. Luo, F. Liu, Y. Zheng, Y. Xiao, Y. Cao, C. Au, S. Liang and L. Jiang, *Green Energy Environ.*, 2020, doi:10.1016/j.gee.2020.12.016.
- (S2) C. Petit, B. Mendoza and T. J. Bandosz, *ChemPhysChem*, 2010, **11**, 3678–3684.
- (S3) J. N. Joshi, G. Zhu, J. J. Lee, E. A. Carter, C. W. Jones, R. P. Lively and K. S. Walton, *Langmuir*, 2018, **34**, 8443–8450.
- (S4) M. Sheikh Alivand, N. H. M. Hossein Tehrani, M. Shafiei-alavijeh, A. Rashidi, M. Kooti, A. Pourreza and S. Fakhraie, *J. Environ. Chem. Eng.*, 2019, **7**, 102946.
- (S5) G. Nickerl, M. Leistner, S. Helten, V. Bon, I. Senkowska and S. Kaskel, *Inorg. Chem. Front.*, 2014, **1**, 325–330.
- (S6) X. Liu and R. Wang, *J. Hazard. Mater.*, 2017, **326**, 157–164.
- (S7) H.-L. Tran, M.-S. Kuo, W.-D. Yang and Y.-C. Huang, *Adsorpt. Sci. Technol.*, 2016, **34**, 275–286.
- (S8) L. Barelli, G. Bidini, L. Micoli, E. Sisani and M. Turco, *Energy*, 2018, **160**, 44–53.
- (S9) A. H. Abdullah, R. Mat, S. Somderam, A. S. Abd Aziz and A. Mohamed, *J. Ind. Eng. Chem.*, 2018, **65**, 334–342.
- (S10) S. Rezaei, M. O. D. Jarligo, L. Wu and S. M. Kuznicki, *Chem. Eng. Sci.*, 2015, **123**, 444–449.
- (S11) C. Liu, R. Zhang, S. Wei, J. Wang, Y. Liu, M. Li and R. Liu, *Fuel*, 2015, **157**, 183–190.
- (S12) S.-K. Lee, Y.-N. Jang, I.-K. Bae, S.-C. Chae, K.-W. Ryu and J.-K. Kim, *Mater. Trans.*, 2009, **50**, 2476–2483.